Identification of immune-related genes and development of a prognostic model in mantle cell lymphoma

Wei Zhang[1#], Jin-Ning Shi[1#], Hai-Ning Wang[2], Ting Zhang[1], Xuan Zhou[1], Hong-Mei Zhang[3], Feng Zhu[3]

[1]Department of Hematology, The Affiliated Jiangning Hospital of Nanjing Medical University, Nanjing, China; [2]Department of Blood Supply, Nanjing Red Cross Blood Center, Nanjing, China; [3]Department of Blood Transfusion, The Affiliated Jiangning Hospital of Nanjing Medical University, Nanjing, China

Contributions: (I) Conception and design: W Zhang, HM Zhang, F Zhu; (II) Administrative support: F Zhu, JN Shi, HM Zhang; (III) Provision of study methods: W Zhang, X Zhou, HM Zhang; (IV) Collection and assembly of data: W Zhang, HN Wang, X Zhou, T Zhang; (V) Data analysis and interpretation: W Zhang, HN Wang, T Zhang, X Zhou; (VI) Manuscript writing: All authors; (VII) Final approval of manuscript: All authors.

[#]These authors contributed equally to this work.

Correspondence to: Feng Zhu; Hong-Mei Zhang. Department of Blood Transfusion, The Affiliated Jiangning Hospital of Nanjing Medical University, Nanjing 211100, China. Email: zhm.0619@163.com; zhm.0619@126.com.

Background: The immune landscape, prognostic model, and molecular variations of mantle cell lymphoma (MCL) remain unclear. Hence, an integrated bioinformatics analysis of MCL datasets is required for the development of immunotherapy and the optimization of targeted therapies.

Methods: Data were obtained from the Gene Expression Omnibus (GEO) database (GSE32018, GSE45717 and GSE93291). The differentially expressed immune-related genes were selected, and the hub genes were screened by three machine learning algorithms, followed by enrichment and correlation analyses. Next, MCL molecular clusters based on the hub genes were identified by K-Means clustering, the probably approximately correct (PAC) algorithm, and principal component analysis (PCA). The landscape of immune cell infiltration and immune checkpoint molecules in distinct clusters was explored by single-sample gene-set enrichment analysis (ssGSEA) as well as the CIBERSORT and xCell algorithms. The prognostic genes and prognostic risk score model for MCL clusters were identified by least absolute shrinkage and selection operator (LASSO)-Cox analysis and cross-validation for lambda. Correlation analysis was performed to explore the correlation between the screened prognostic genes and immune cells or immune checkpoint molecules.

Results: Four immune-related hub genes (*CD247*, *CD3E*, *CD4*, and *GATA3*) were screened in MCL, mainly enriched in the T-cell receptor signaling pathway. Based on the hub genes, two MCL molecular clusters were recognized. The cluster 2 group had a significantly worse overall survival (OS), with down-regulated hub genes, and a variety of activated immune effector cells declined. The majority of immune checkpoint molecules had also decreased. An efficient prognostic model was established, including six prognostic genes (*LGALS2*, *LAMP3*, *ICOS*, *FCAMR*, *IGFBP4*, and *C1QA*) differentially expressed between two MCL clusters. Patients with a higher risk score in the prognostic model had a poor prognosis. Furthermore, most types of immune cells and a range of immune checkpoint molecules were positively correlated with the prognostic genes.

Conclusions: Our study identified distinct molecular clusters based on the immune-related hub genes, and showed that the prognostic model affected the prognosis of MCL patients. These hub genes, modulated immune cells, and immune checkpoint molecules might be involved in oncogenesis and could be potential prognostic biomarkers in MCL.

Keywords: Mantle cell lymphoma (MCL); immune-related genes; prognosis; bioinformatics integration analysis

Submitted Nov 02, 2022. Accepted for publication Dec 08, 2022.

doi: 10.21037/atm-22-5815

View this article at: https://dx.doi.org/10.21037/atm-22-5815

Introduction

Mantle cell lymphoma (MCL), a heterogeneous and invariably aggressive non-Hodgkin lymphoma (NHL), accounts for 5–7% of all lymphomas, with approximately 70% of cases occurring in men and a median patient age of about 60–70 years (1). MCL possesses both indolent and aggressive NHL characteristics, with a median overall survival (OS) of about 3–5 years (2), and inevitably relapses following standard frontline therapies, such as immunochemotherapy and autologous stem cell transplantation (3). Although innovative agents have improved the therapeutic options for MCL patients, the identification of individual risk profiles based on MCL complex biology and the choice of combined targeted therapies remains challenging. Therefore, further understanding of the molecular genetic background and relative prognostic factors of MCL may aid in optimizing treatments and exploring new therapeutic targets.

A series of genetic variations have been reported to participate in the pathogenesis and prognostic prediction of MCL patients. Cyclin D1 overexpression, derived from the t(11;14)(q13;q32) translocation, is the known characteristic change and is accompanied by cell cycle deregulation (4). Several prognostic biomarkers have been identified in MCL: 6 genes (*AKT3*, *BCL2*, *BTK*, *CD79B*, *PIK3CD*, and *SYK*) mostly from the B-cell receptor pathway (5); hub genes, including *KIF11*, *CDC20*, *CCNB1*, *CCNA2*, and *PUF60* (6); and 10 genes (*KIF18A*, *YBX3*, *PEMT*, *GCNA*, *POGLUT3*, *SELENOP*, *AMOTL2*, *IGFBP7*, *KCTD12*, and *ADGRG2*) related to the cell cycle, apoptosis, and metabolism (7). Based on genomic and transcriptomic profiling, four MCL molecular subsets were identified, which affected clinical outcomes and were involved in clonal evolution (8). However, the complex molecular mechanisms in MCL pathogenesis remain largely unexplored.

Cancer immunotherapy has been an effective anti-cancer treatment in recent years, and among them, the groundbreaking immune checkpoint blockade (ICB) therapies have improved the outcomes of patients with different tumors, including classical Hodgkin lymphoma and natural killer (NK)/T-cell lymphoma (9-11). Nevertheless, in the majority of hematological malignancies, the clinical benefit from ICB therapies remains limited, even when used in combination therapy (9,12). In MCL, the effects of various immune checkpoint inhibitors (ICIs) are inconclusive, and the expressions of programmed death 1 (PD-1) and its ligands are almost undetectable (13,14). Moreover, the immune-response genes and stromal microenvironments have confirmed the major roles in the survival, progression, and chemoresistance of MCL (15-17). Therefore, understanding the immune landscape and molecular variations in MCL is essential for the development of immunotherapy. Dufva *et al*. defined the multifaceted immune landscape of various hematological malignancies by integrating the data of genetic and epigenetic aberrations and the tumor microenvironment (TME) (12). A clinical immune-related prognostic model, including the predictors of B symptoms, platelet count, beta-2-microglobulin (β2-MG) level, cluster of differentiation 4 $(CD4)^+$ T-cell count <26.7%, and $CD8^+$ T-cell count >44.2%, could predict the OS of MCL patients (18). However, the immune-related hub genes, prognostic model, and underlying mechanisms of MCL require further elucidation.

In this study, we performed an integrated bioinformatics analysis of MCL datasets from the Gene Expression Omnibus (GEO) database to investigate the immune-related genes, immune infiltrated cells, and immune checkpoint molecules and identify MCL molecular clusters based on the immune-related hub genes. We also established a prognostic risk score model and explored the potential immune cell regulation and relative molecular mechanisms. The flowchart of this study is shown in *Figure 1*. We present the following article in accordance with the TRIPOD reporting checklist (available at https://atm.

Highlight box

Key findings

- The distinct molecular clusters based on immune-related hub genes were identified, and a prognostic model was established in MCL.

What is known and what is new?

- Innovative agents have improved the therapeutic options for MCL patients, however, the immune checkpoint blockade therapies remain limited.
- This study identified the immune-related hub genes and a prognostic model of MCL, and preliminary explored the potential immune cell regulation and relative molecular mechanisms.

What is the implication, and what should change now?

- The immune-related hub genes, modulated immune cells, and immune checkpoint molecules might be involved in oncogenesis and could be potential prognostic biomarkers in MCL. Further research should be carried out to examine the regulatory mechanisms and explore the efficiency of the prognostic model, for enhancing the effect of immunotherapy.

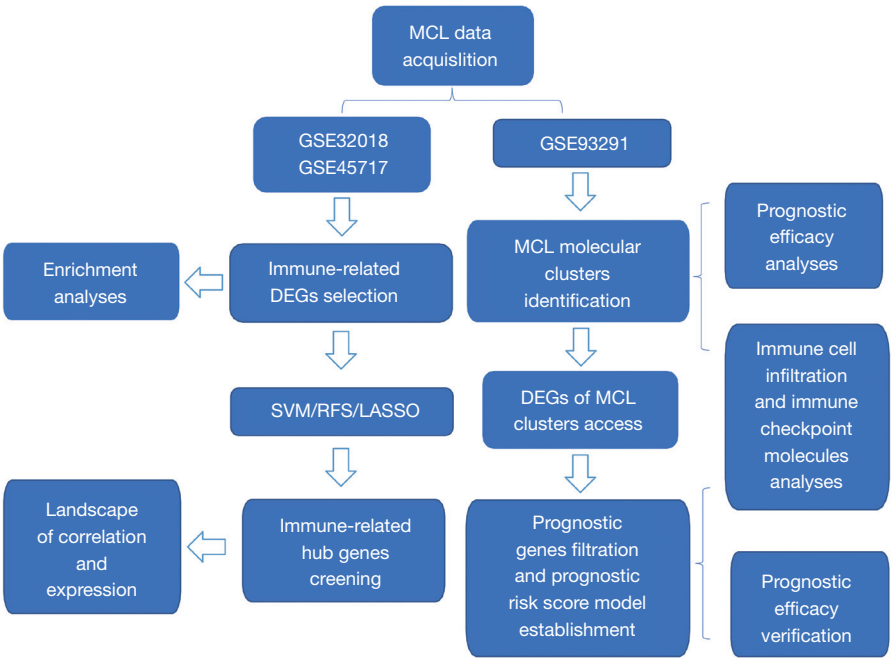

Figure 1 Study flowchart. MCL, mantle cell lymphoma; DEGs, differentially expressed genes; SVM, SVM-RFE, support vector machine-recursive feature elimination; RFS, Random forest; LASSO, least absolute shrinkage and selection operator.

amegroups.com/article/view/10.21037/atm-22-5815/rc).

Methods

Data selection and acquisition

The study was conducted in accordance with the Declaration of Helsinki (as revised in 2013). The data in this study was respectively obtained from GSE32018 (19), GSE45717 (20), and GSE93291 (21) datasets in the GEO database (http://www.ncbi.nlm.nih.gov/geo). There were 24 tumor samples and seven normal controls in GSE32018, five tumor samples and eight normal controls in GSE45717, and 123 tumor samples in GSE93291.

Expression and enrichment analyses of immune-related genes in MCL

The immune-related genes were obtained and downloaded from the GeneCards database (http://www.genecards.org/), using a keyword search of the term "immune". Using the "limma (v3.42.2)" in R software package (https://www.r-project.org/), the differentially expressed genes (DEGs) were selected between MCL tumor samples and normal controls in the GSE32018 and GSE45717 datasets. The threshold was defined as follows: adjusted P value <0.05 and |log fold change (FC)| >0.585. The common DEGs were selected and visualized via "Venn Diagram (v1.7.3)" in R package. For the Gene Ontology (GO) and Kyoto Encyclopedia of Genes and Genomes (KEGG) enrichment analyses, functional and pathway enrichment analyses of the common DEGs were performed using "clusterProfiler (v4.0)" in R package, using P<0.05 and q<0.2 as the threshold.

Screening of immune-related hub genes in MCL

The hub DEGs in MCL, which could distinguish cancerous from normal tissue, were screened in the much larger GSE32018 dataset, using three machine learning algorithms, respectively. Firstly, the hub genes were acquired using the support vector machine-recursive feature elimination (SVM-RFE) algorithm (https://github.com/johncolby/SVM-RFE) via 10-fold cross-validation.

Secondly, the hub genes were obtained by a random forest algorithm using the "RandomForest (v4.6-14)" R package, using ntree =50, and MeanDecreaseGini >0 as the threshold. Thirdly, the hub genes were selected through the least absolute shrinkage and selection operator (LASSO) algorithm using "glmnet (v4.0-2)" R package via 10-fold cross-validation for lambda. Finally, the common hub

genes from three algorithms were demonstrated by the "Venn Diagram (v1.7.3)" R package. The String database (https://cn.string-db.org/) was employed for protein-protein interaction (PPI) network analysis and functional enrichment analysis of these hub genes. The correlation among these genes was determined via Pearson's correlation analysis.

The location information of the screened immune-related hub genes was displayed in a circos ideogram using "RCircos (v1.2.1)" R package. In the GSE32018 database, the correlation between these genes was demonstrated by Pearson's correlation analysis, and scatter plots were utilized to display the gene pairs, using |correlation| >0.6. The expression of these genes between the cancer and normal samples was presented via a heatmap and scatter plot.

Identification of MCL molecular clusters based on the immune-related hub genes

The expression matrix of immune-related hub genes in the GSE93291 dataset was analyzed by K-Means clustering using the "ConsensusClusterPlus (v1.50.0)" R package. The molecular clusters of MCL were recognized via the probably approximately correct (PAC) algorithm, and Kaplan-Meier survival analysis was performed. Principal component analysis (PCA) was conducted using "factoextra (v1.0.7)" and "FactoMineR (v2.4)" R packages. The expression of these hub genes in distinct molecular clusters was displayed in a boxplot and heatmap.

The landscape of immune cell infiltration and immune checkpoint molecules in distinct MCL molecular clusters based on the immune-related hub genes

The distinct MCL molecular clusters based on the immune-related hub genes in the GSE93291 dataset was analyzed using hallmark gene sets in the Molecular Signature Database (MSigDB) (https://www.gsea-msigdb.org/gsea/msigdb/, MSigDB v7.5.1) via single-sample gene-set enrichment analysis (ssGSEA). The differences were detected using the wilcox.test R package.

Immune cell infiltration in the TME of MCL molecular clusters was revealed by the ImmuneScore, StromalScore, ESTIMATEScore, and TumorPurity using the "ESTIMATE (v1.0.13)" R package. The differences were detected using the wilcox.test R package. Next, the enrichment scores of immune infiltrating cells were calculated by the ssGSEA algorithm via the gene set variation analysis (GSVA) (v1.34.0) R package. In addition, immune cell infiltration was explored using the "CIBERSORT (v1.03)" and "xCell (v1.1.0)" R packages, respectively, and the differences were detected using the wilcox.test R package. The expression levels of familiar immune checkpoint molecules in the distinct MCL molecular clusters were displayed in a boxplot, and the differences were detected using the wilcox.test R package.

Identification of prognostic genes and development of a prognostic risk score model for distinct MCL molecular clusters

The DEGs of distinct MCL molecular clusters in the GSE93291 dataset were obtained using the "limma (v3.42.2)" R package. The threshold was defined as follows: adjusted P<0.05 and |logFC| >1. The prognostic genes were identified via LASSO-Cox analysis, followed by univariate Cox regression analysis of the DEGs that were significantly correlated with the OS of MCL patients, with a cut-off value of P<0.05. The prognostic risk score model was established by the screened prognostic genes using the "glmnet (v4.0-2)" R package via cross-validation for lambda. The minimum of 1-standard error of λ was employed, and the maxit was set to 1,000. The screened prognostic genes with non-zero coefficients were performed by multivariate Cox regression to calculate relative risk scores, using the enter method. The risk score of each sample was calculated using the following formula:

$$\mathrm{RScore}_i = \sum_{j=1}^{n} \exp_{ji} \times \beta_j \quad [1]$$

where exp refers to the expression level of the relative gene, β denotes the regression coefficient (coef) of the relative gene in LASSO regression, Rscore represents the risk score in each sample, *n* is the number of screened prognostic genes, *i* is the sample, and *j* is the gene.

To verify the efficiency of the prognostic risk score model, we performed a Kaplan-Meier survival analysis to compare the difference in OS between the high- and the low-risk score groups, as distinguished by the median Rscore in the GSE93291 dataset. Subsequently, the receiver operating characteristic (ROC) curve and area under the curve (AUC) was used to assess the prognostic model.

Correlation between the screened prognostic genes and immune cell infiltration or immune checkpoint molecules in distinct MCL molecular clusters

The correlation between the screened prognostic genes in the GSE93291 dataset and immune infiltrating cells was demonstrated via Pearson's correlation analysis. In addition, a similar correlation analysis was performed between the prognostic genes and familiar immune checkpoint molecules.

Statistical analysis

Statistical analysis was performed using related R software packages and the bioinformatics databases mentioned above. The Wilcoxon test was utilized to compare two independent non-parametric samples. Survival analysis was performed using the log-rank test. The screened genes correlated with the relative cells or molecules were evaluated using Pearson's correlation test. $P<0.05$ was considered statistically significant.

Results

Expression and enrichment analyses of immune-related genes in MCL

A total of 818 immune-related genes with a relevance score ≥5 were retrieved from the GeneCards database (available at: https://cdn.amegroups.cn/static/public/atm-22-5815-1.xlsx). In the GSE32018 dataset, 722 immune-related genes had available expression data, including 193 DEGs between the MCL tumor and the normal samples (*Figure 2A*, Table S1). In the GSE45717 dataset, 677 immune-related genes had available expression information and there were 211 DEGs (*Figure 2B*, Table S2). There were a total of 77 common DEGs in the GSE32018 and GSE45717 datasets (*Figure 2C*). Functional and pathway enrichment analyses of the common genes showed that they were mainly enriched in T-cell activation, leukocyte cell-cell adhesion, and the regulation of immune cell proliferation via GO analysis of the biological processes (BP); in the external side of the plasma membrane, plasma membrane receptor complex, and the membrane raft via GO analysis of the cellular components (CC); in cytokine receptor binding/activity, cytokine binding/activity, and tumor necrosis factor receptor (superfamily)/major histocompatibility complex (MHC) protein binding via GO analysis of the molecular functions (MF); as well as in cytokine-cytokine receptor interaction, hematopoietic cell lineage, T helper cell 17 (Th17) cell differentiation, T cell receptor signaling pathway, nuclear factor kappa-B (NF-κB) signaling pathway, programmed death-ligand 1 (PD-L1) expression, and the PD-1 checkpoint pathway in cancer via KEGG analysis (*Figure 2D-2G*).

Screening of immune-related hub genes in MCL

By screening the 77 common DEGs, we obtained the immune-related hub genes in MCL using three machine learning algorithms in the GSE32018 dataset. Firstly, the top nine most accurate genes were selected via 10-fold cross-validation by SVM-RFE (*Figure 3A*). The average rankings of the 77 genes are displayed in Table S3. Next, 26 genes were selected via MeanDecreaseGini using a random forest (*Figure 3B,3C*, Table S4). Then, 11 genes with a low mean-squared error were obtained via lasso.min using a LASSO algorithm (*Figure 3D*). Finally, the immune-related hub genes among the three algorithms in MCL were demonstrated using a Venn diagram (*Figure 3E*).

The four common hub genes (*CD247*, *CD3E*, *CD4*, and *GATA3*) were screened for further analyses. PPI network analysis demonstrated an interaction between these genes. GO enrichment analysis revealed that they were mainly enriched in the T-cell receptor signaling pathway (GO:0050852), T-cell selection (GO:0045058), the regulation of interleukin-2 (IL-2) production (GO:0032663), the adaptive immune response (GO:0002250), and cytokine production (GO:0001816). The expression of these four genes exhibited a positive correlation (*Figure 3F,3G*).

The location of the four screened hub genes in the human chromosome is shown in *Figure 4A*. Pearson's correlation analysis indicated that *CD247*, *CD3E*, and *CD4* had a significant positive relationship with $|correlation| >0.6$ (*Figure 4B*). The four hub genes in GSE32018 were also displayed in a volcano plot (*Figure 4C*); the expression of these genes in the tumor samples was markedly lower than that in the normal samples (*Figure 4D,4E*).

Identification of MCL molecular clusters based on the immune-related hub genes in MCL

Two MCL molecular clusters were recognized via a PAC algorithm in the GSE93291 dataset, followed by the unsupervised clustering of the expression matrix of four immune-related hub genes (*Figure 5A-5D*). The MCL patients in molecular cluster 2 had worse OS compared

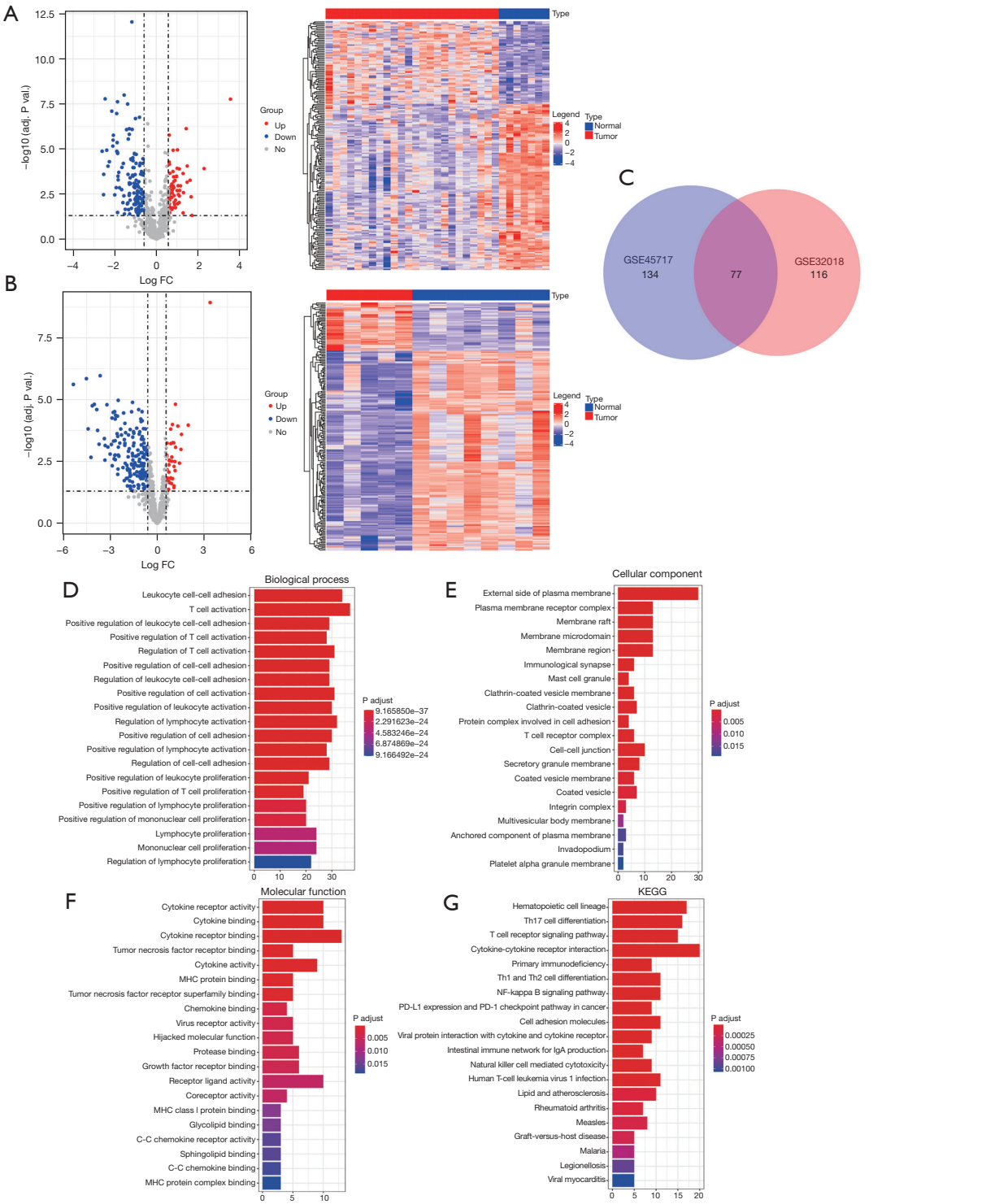

Figure 2 The immune-related genes in MCL. (A,B) Volcano plot and heatmap of 193 DEGs in GSE32018 and 211 DEGs in GSE45717. (C) Venn diagram of DEGs in GSE32018 and GSE45717. (D-F) GO analysis (BP, CC, and MF) of the 77 common genes. (G) KEGG analysis of the 77 common genes. The x-axis in 2D-2G represented –log10 (adjusted P value), respectively. FC, fold change; KEGG, Kyoto Encyclopedia of Genes and Genomes; PD-L1, programmed death-ligand 1; PD-1, programmed death 1; MCL, mantle cell lymphoma; DEGs, differentially expressed genes; GO, Gene Ontology; BP, biological processes; CC, cellular components; MF, molecular functions.

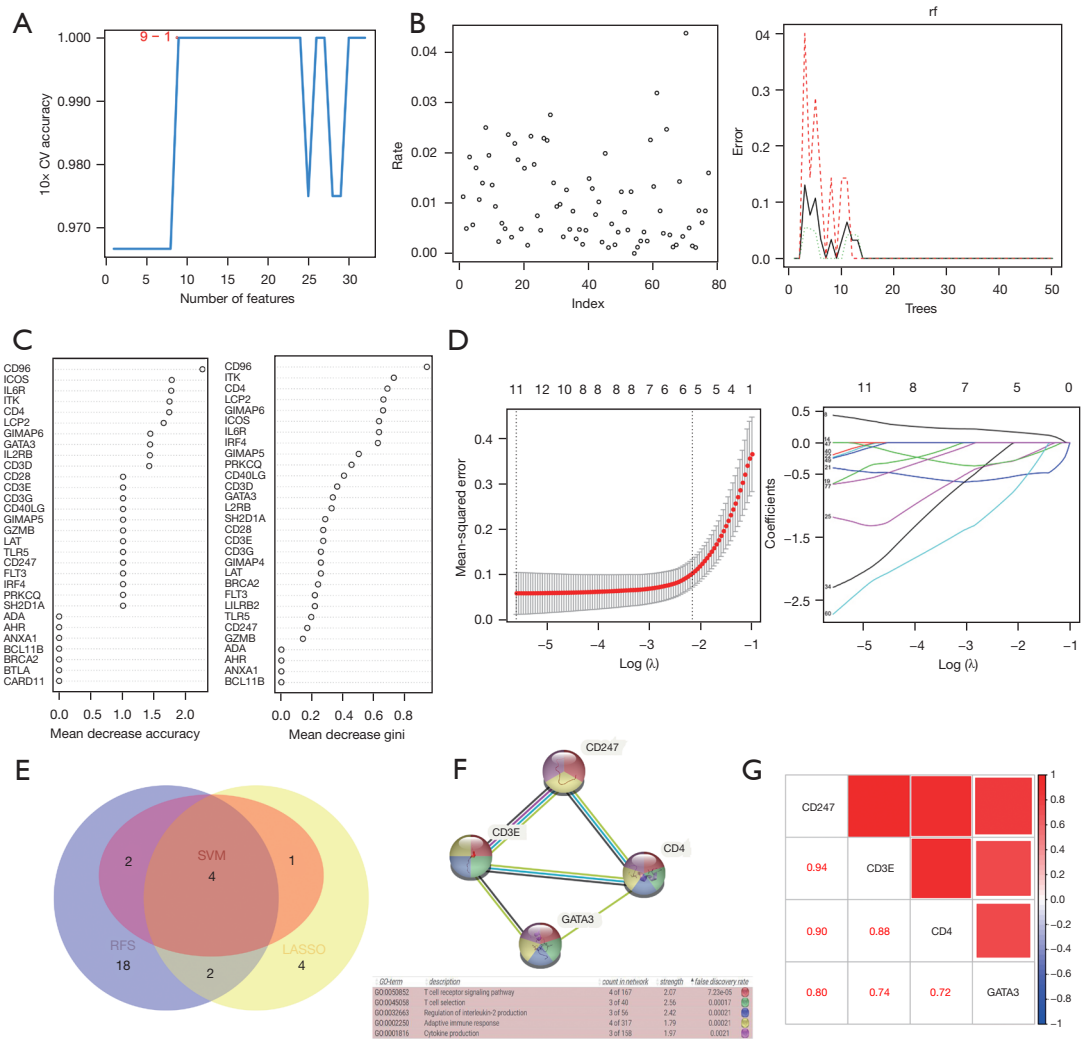

Figure 3 The screening of immune-related hub genes in MCL (GSE32018). (A) The accuracy of the 77 common DEGs by SVM-RFE. (B) Error in the screening process using a random forest algorithm. (C) The MeanDecreaseAccuracy and MeanDecreaseGini of hub genes using a random forest algorithm. (D) The coefficient of lambda and the lambda.min from 10-fold cross-validation using a LASSO algorithm. (E) Venn diagram of hub genes in three machine learning algorithms (SVM, SVM-RFE; RFS). (F) PPI network and GO analysis of the four hub genes. (G) Correlation among the four hub genes. CV, cross-validation; RFS, Random forest; SVM, SVM-RFE, support vector machine-recursive feature elimination; GO, Gene Ontology; MCL, mantle cell lymphoma; DEGs, differentially expressed genes; LASSO, least absolute shrinkage and selection operator; PPI, protein-protein interaction.

with those in cluster 1 (P=0.042) (*Figure 5E*). The overall expression of these hub genes in cluster 2 was lower than that in cluster 1 (*Figure 5F,5G*).

The landscape of immune cell infiltration and immune checkpoint molecules in distinct MCL molecular clusters

A total of 26 out of 50 pathways of hallmark gene sets exhibited differences between the two MCL molecular clusters in the GSE93291 dataset. The top 10 alterative pathways included: APICAL_JUNCTION, APICAL_SURFACE, ALLOGRAFT_REJECTION, WNT_BETA_CATENIN_SIGNALING, IL6_JAK_STAT3_SIGNALING, INTERFERON_GAMMA_RESPONSE, HEDGEHOG_SIGNALING, MYC_TARGETS_V1, INFLAMMATORY_RESPONSE, and OXIDATIVE_

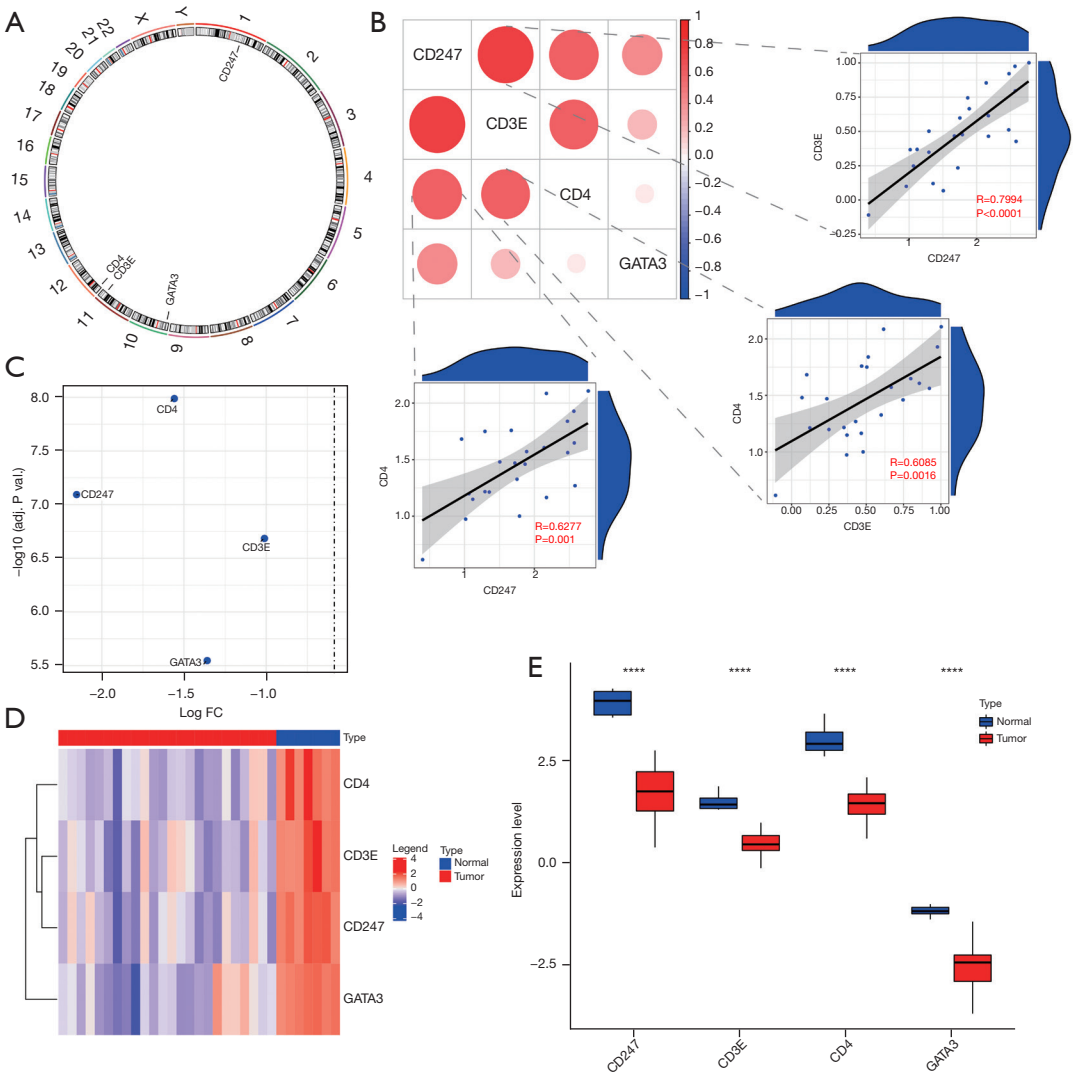

Figure 4 The landscape of immune-related hub genes in MCL (GSE32018). (A) The chromosome location of the four hub genes. (B) Correlation among the hub genes. (C) Volcano plot of the hub genes. (D,E) Expression of the hub genes in the tumor and normal samples. ****, P<0.0001. FC, fold change; MCL, mantle cell lymphoma.

PHOSPHORYLATION (*Figure 6A*).

Compared with those in cluster 1, the ImmuneScore and ESTIMATEScore were lower in the cluster 2 group, while the TumorPurity scores were higher (*Figure 6B,6C*). A total of 18 of 28 immune cell infiltrations in the TME had different scores between the two clusters. The activated $CD8^+$ T cell, activated dendritic cell, natural killer T cell, and T follicular helper cell scores in cluster 2 were significantly lower than that in cluster 1 (*Figure 6D*). Similar differences were observed in the immune cell proportion of two clusters, which were analyzed by CIBERSORT and xCell, respectively (Figure S1A,S1B).

Forty-one of the 63 familiar immune checkpoint molecules had available expression information in the GSE93291 dataset (Table S5). The data showed that 25 immune checkpoint molecules had different expression levels in the two MCL clusters. Compared with cluster 1, only *CD86* was higher in cluster 2, while the other 24 molecules were lower, especially *BTN3A1*, *BTN3A2*, *BTN3A3*, *CD200*, *CD274*, *CD28*, *ICOS*, *IDO1*, *IL2RB*, and

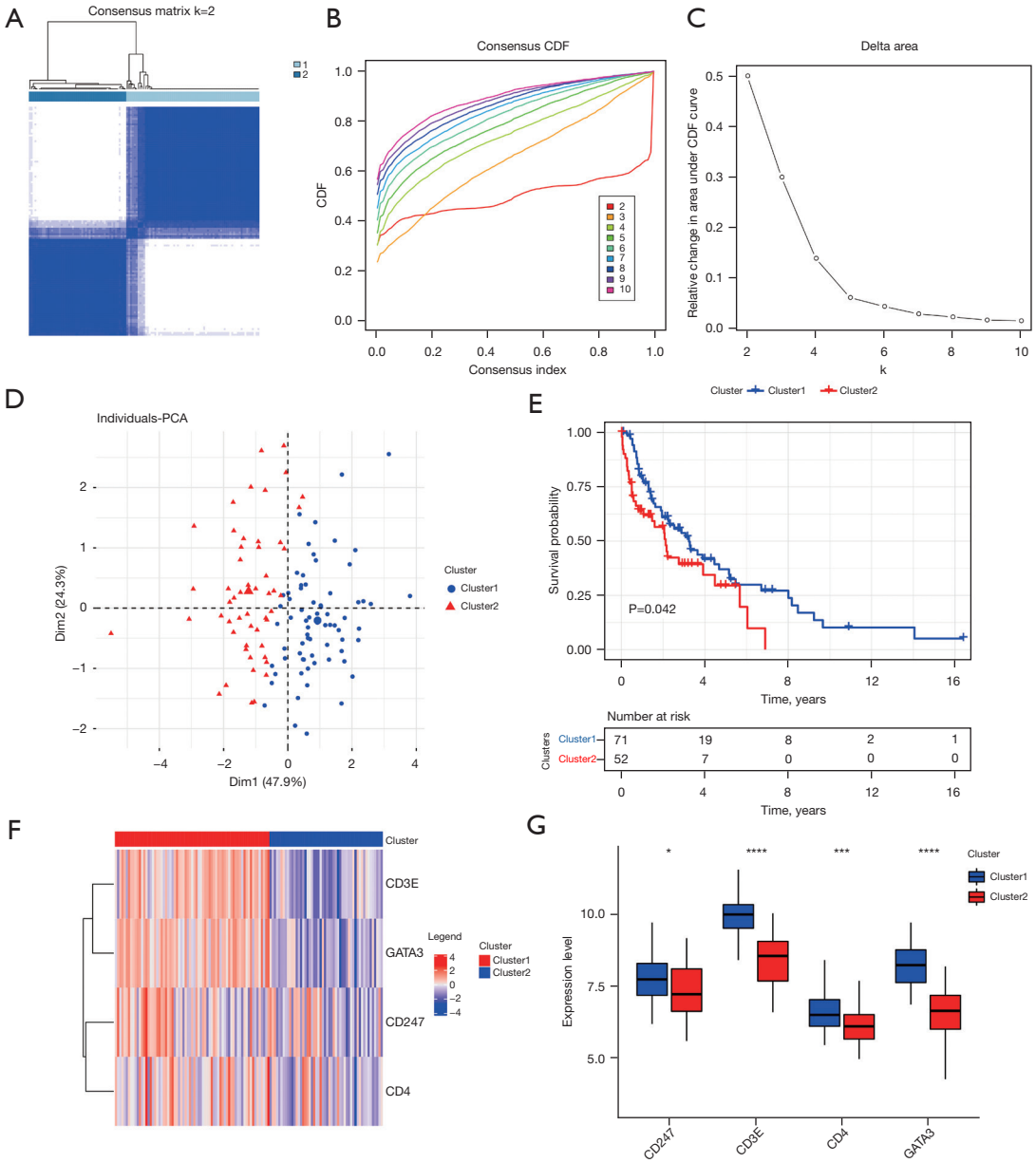

Figure 5 Identification of MCL molecular clusters in MCL (GSE93291). (A-C) Two MCL molecular clusters were classified by unsupervised clustering and displayed using a heatmap, CDF plot, and macadam plot. (D) Analysis of MCL samples in two clusters by PCA. (E) Prognostic OS differences between the two clusters. (F,G) Expression of the four immune-related hub genes in the two clusters. ****, P<0.0001; ***, P<0.001; *, P<0.05. CDF, cumulative distribution function; PCA, principal component analysis; MCL, mantle cell lymphoma; OS, overall survival.

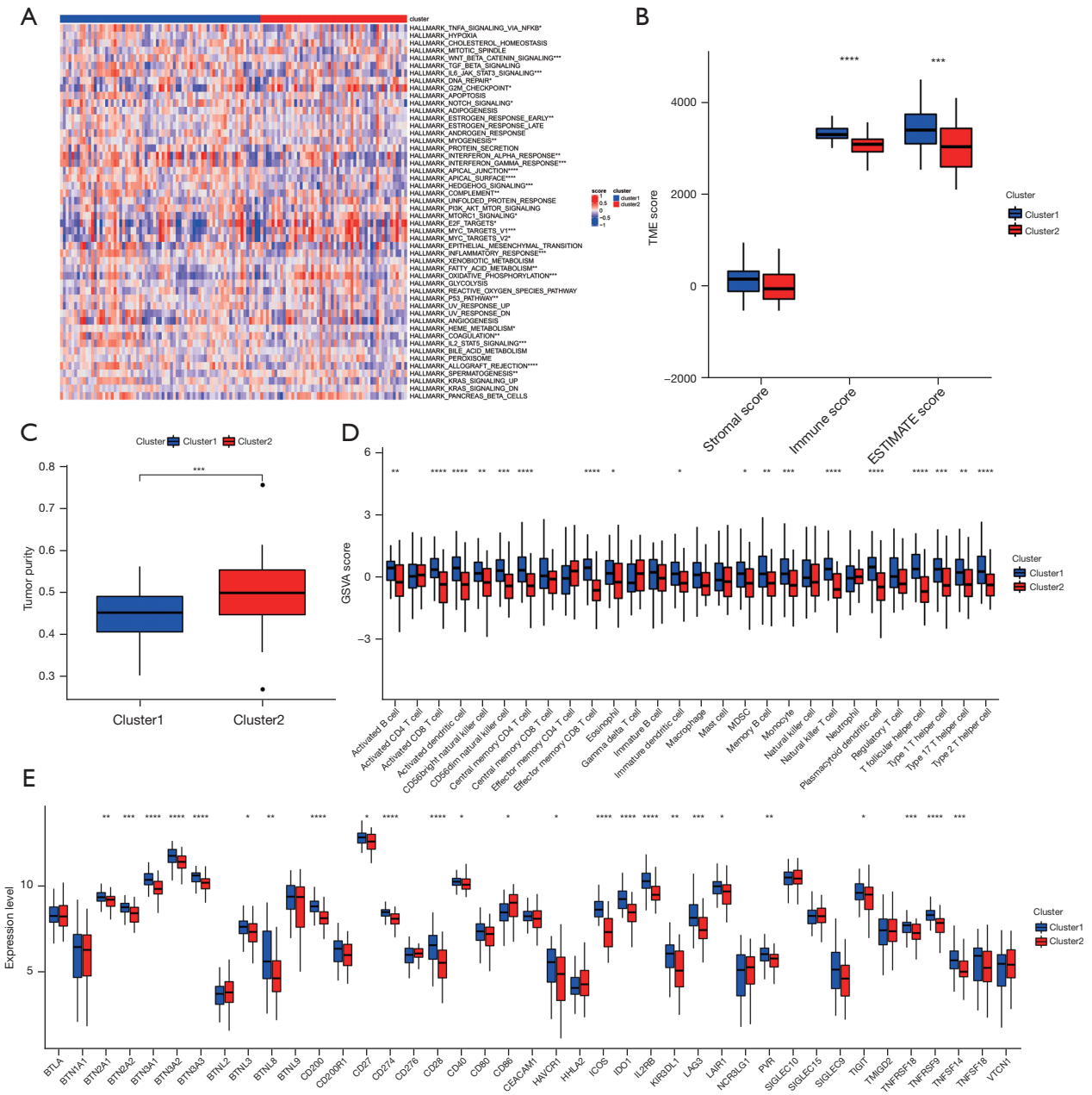

Figure 6 The landscape of immune cell infiltration and immune checkpoint molecules in the MCL molecular clusters (GSE93291). (A) Enrichment analysis of the pathways of hallmark gene sets in the two MCL clusters. (B,C) The ImmuneScore, StromalScore, ESTIMATEScore, and TumorPurity scores in the MCL samples of the two clusters. (D) The scores of 28 immune cell infiltrations in the TME of the two clusters were calculated by ssGSEA via GSVA. (E) The expression of 41 immune checkpoint molecules in the two clusters. ****, P<0.0001; ***, P<0.001; **, P<0.01; *, P<0.05. TME, tumor microenvironment; MCL, mantle cell lymphoma; ssGSEA, single-sample gene-set enrichment analysis; GSVA, gene set variation analysis.

TNFRSF9 (*Figure 6E*).

Identification of the prognostic genes and development of the prognostic risk score model for distinct MCL molecular clusters

In order to explore the prognostic DEGs of the two MCL molecular clusters, the 65 DEGs of the two clusters and coding relative proteins were obtained in the GSE93291 dataset (Table S6), and the 20 DEGs significantly associated with the OS of MCL patients were screened by univariate Cox regression analysis (Table S7). Then, six DEGs (*LGALS2*, *LAMP3*, *ICOS*, *FCAMR*, *IGFBP4*, and *C1QA*) were selected to establish the prognostic risk score model via LASSO-Cox analysis (*Figure 7A-7C*). The poor OS was related to the increased *IGFBP4* and *C1QA* expression groups; however, it was more likely to occur in the low *LGALS2*, *LAMP3*, *ICOS*, and *FCAMR* expression groups (P<0.05). The following formula was used: Risk Score = *LGALS2* × (–0.1746) + *LAMP3* × (–0.1413) + *ICOS* × (–0.1352) + *FCAMR* × (–0.1327) + *IGFBP4* × 0.0356 + *C1QA* × 0.1987. MCL patients who had a higher prognostic model risk score had a poorer prognosis, as verified by Kaplan-Meier survival analysis (P<0.0001) (*Figure 7D*). The AUCs at 1, 3, and 5 years were 0.8, 0.79, and 0.7, respectively (*Figure 7E*). Taken together, these results demonstrated that the prognostic model had a prominent efficiency.

Correlation between the screened prognostic genes and immune cell infiltration or immune checkpoint molecules for distinct MCL molecular clusters

The six screened prognostic genes (*LGALS2*, *LAMP3*, *ICOS*, *FCAMR*, *IGFBP4*, and *C1QA*) were correlated with the majority of the 28 immune infiltrating cells. Immune cells that were significantly positively correlated with the whole six prognostic genes were activated in $CD8^+$ T cells, effector memory $CD8^+$ T cells, natural killer T cells, and type 1 T helper cells. *IGFBP4* was negatively correlated with effector memory $CD4^+$ T cells and gamma delta T cells, while *C1QA* was negatively correlated with immature B cells (*Figure 8A*). Most of the immune checkpoint molecules were also correlated with the six prognostic genes. Also, a significant positive correlation with the whole six prognostic genes was observed in *ICOS*, *CD200*, *TNFRSF9*, *IL2RB*, *CD274*, and *BTN3A1* (*Figure 8B*).

Discussion

In the present study, we initially compared 77 immune-related differentially expressed genes (DEGs) in MCL samples with normal controls in both the GSE32018 and GSE45717 datasets. These genes were mainly enriched in T-cell activation, the plasma membrane, and cytokine receptor binding and activity by GO analysis, and in a series of pathways by KEGG analysis, including cytokine-cytokine receptor interaction and the NF-kappa B signaling pathway. A previous study showed that these two pathways were enriched in DEGs both in the GSE32018 and GSE9327 datasets, which used normal and reactive lymph nodes as controls, respectively (22). This indicates that the enriched pathways in DEGs between tumor samples and controls might be a reason for the selection of targeted agents in MCL, such as bortezomib interfering with the NF-kappa B signaling pathway (1).

We then screened four common hub genes (*CD247*, *CD3E*, *CD4*, and *GATA3*) using three machine learning algorithms: SVM-RFE, random forest, and LASSO. Previous studies have revealed the biological functions and application prospects of these genes. *CD247*, which encodes the CD3ζ protein, regulates the immune response and participates in tumorigenesis (23). *CD3E*, which encodes the CD3-epsilon polypeptide, is a built-in multifunctional signal tuner in T-cell development (24). *CD4*, which encodes the CD4 membrane glycoprotein, assists the germinal center reaction and contributes to the activation, functions, and longevity of $CD8^+$ T-cells and B-cells (25). *GATA3*, which encodes a protein of the GATA family of transcription factors, is an important regulator of T-cell development and may be a biomarker associated with poor prognosis in distinct subtypes of nodal peripheral T-cell lymphoma (26). We found that the hub genes were mainly enriched in the T-cell receptor signaling pathway, T-cell selection, the regulation of IL-2 production, the adaptive immune response, and cytokine production. These relative pathways were consistent with previous research (22). Moreover, *CD247*, *CD3E*, and *CD4* exhibited a positive relationship with each other. Also, the whole expression of hub genes in MCL was significantly lower than that in the normal samples. These findings suggested that the reduced expression of the four immune-related hub genes, which were related to a series of immune signaling pathways, might participate in MCL tumor progression.

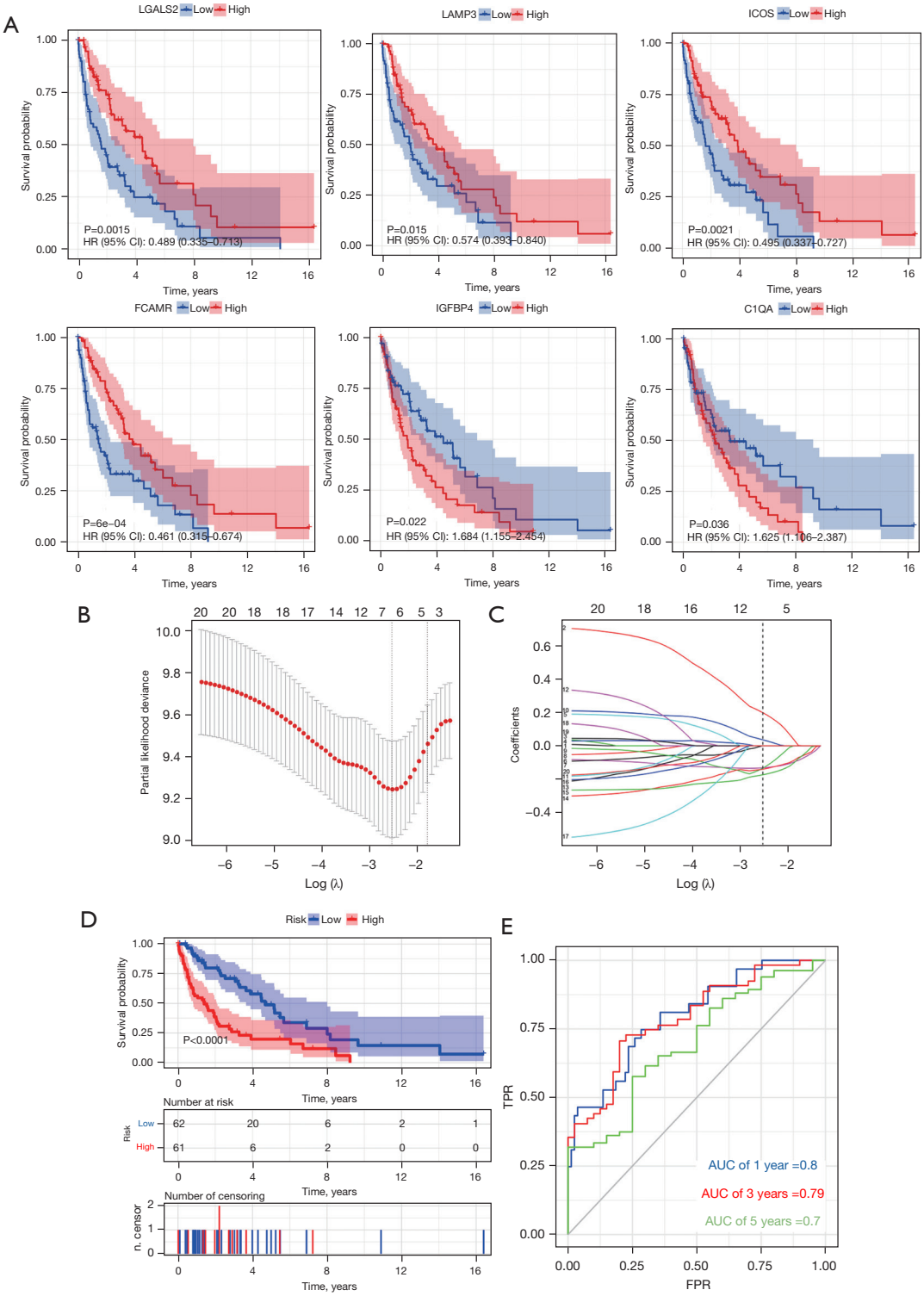

Figure 7 The prognostic genes and prognostic risk score model for the MCL molecular clusters (GSE93291). (A) Prognostic value of the expression of six DEGs (*LGALS2*, *LAMP3*, *ICOS*, *FCAMR*, *IGFBP4*, and *C1QA*) in the MCL samples. (B,C) The prognostic risk score model was established by LASSO-Cox analysis. (D,E) The efficiency of the prognostic model was verified by Kaplan-Meier and ROC curve analysis. HR, hazard ratio; AUC, area under the curve; TPR, true positive rate; FPR, false positive rate; MCL, mantle cell lymphoma; LASSO, least absolute shrinkage and selection operator; ROC, receiver operating characteristic.

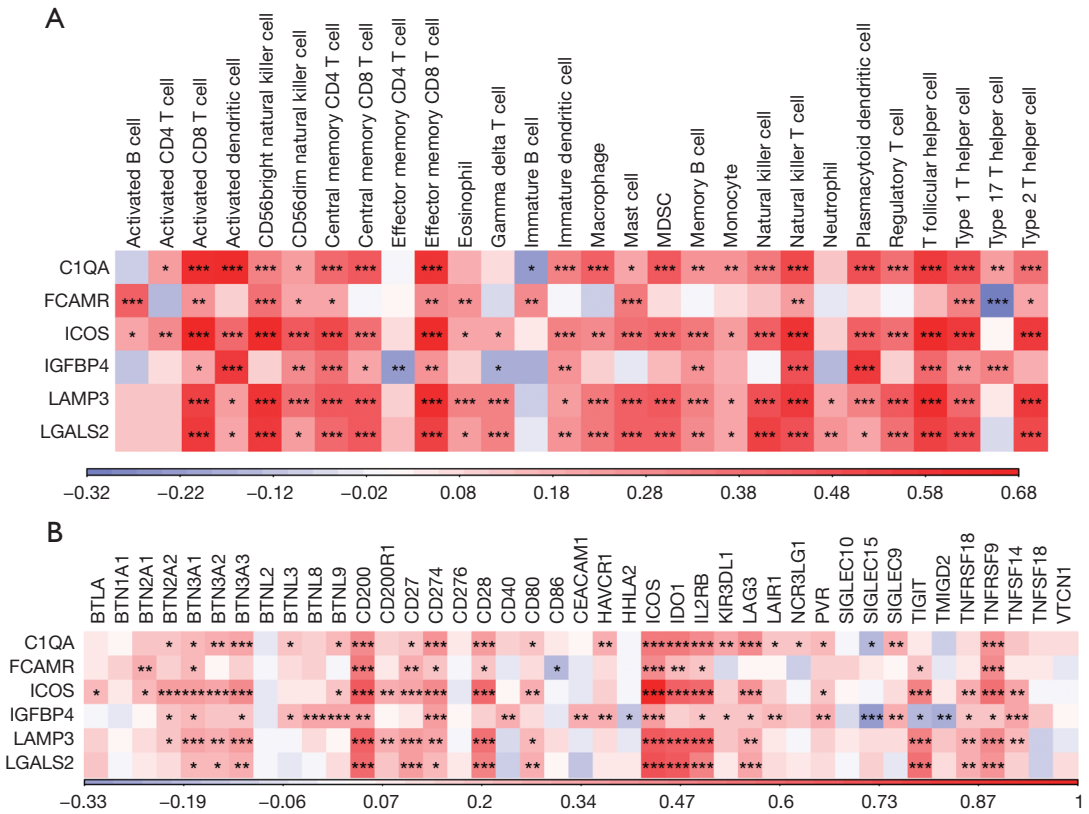

Figure 8 Correlation between the screened prognostic genes and the immune infiltrating cells or immune checkpoint molecules in MCL (GSE93291). (A,B) The correlation between the six prognostic genes and the immune infiltrating cells or immune checkpoint molecules. ***, P<0.001; **, P<0.01; *, P<0.05. MCL, mantle cell lymphoma.

A previous study observed that fewer immune escape genes, which are significantly expressed in diffuse large B-cell lymphoma and follicular lymphoma, were enriched in MCL samples (27). To further identify the four screened hub genes, we utilized unsupervised clustering of the expression matrix of hub genes and recognized two MCL molecular clusters in the much larger GSE93291 dataset. Interestingly, the patients in cluster 2 had a significantly worse OS and lower expression of the whole hub genes, compared with those in cluster 1. This indicated that the down-regulated expression of the four hub genes was unfavorable to the prognosis of MCL patients. Furthermore, we explored the landscape of immune cell infiltration and immune checkpoint molecules in the two MCL clusters. Several different pathways of hallmark gene sets were explored between the two clusters. The results were consistent with previous research on the immune landscape of MCL in terms of the cytolytic score-related pathways, including INTERFERON_GAMMA_RESPONSE, ALLOGRAFT_REJECTION, and INFLAMMATORY_RESPONSE (12). However, using the different classification methods from a recent study, which classified MCL into four clusters by whole-exome sequencing and relatively matched RNA sequencing (RNA-Seq) data analysis (8), we also found that the active MYC pathway was involved in the MCL progression.

Moreover, we observed that several immune scores reflecting the immune cell infiltration in the TME were different between the two MCL clusters. In cluster 2, the activated $CD8^+$ T-cells, activated dendritic cells, natural killer T cells, and T follicular helper cells exhibited significantly lower scores. This indicated that a variety of activated immune effector cells were lower in cluster 2. Previous studies have shown that the various characteristics of immune cell infiltration affected MCL outcomes. Zhang *et al.* discovered the progressive dampening of $CD8^+$ T cells in refractory MCL patients (28). The low absolute $CD4^+$ T cell counts in peripheral blood were a significant predictor

of unfavorable OS in MCL patients, regardless of whether they received rituximab treatment (29). Similarly, we found that central memory $CD4^+$ T cells were decreased in cluster 2, with a poor outcome. Rodrigues *et al.* reported that the infiltrations of CD163-, PD-L1-, and FoxP3-positive cells were indicative of a worse outcome in MCL patients, independent of established risk factors (30).

In this study, only *CD86* was higher among the 25 differentially expressed immune checkpoint molecules in cluster 2, as compared with cluster 1. Also the most significantly decreased molecules were *BTN3A1*, *BTN3A2*, *BTN3A3*, *CD200*, *CD274*, *CD28*, *ICOS*, *IDO1*, *IL2RB*, and *TNFRSF9*. Previous studies have evaluated the expression of several immune checkpoint molecules and explored their effects on the prognosis of MCL and other B-cell lymphomas. The addition of heterodimeric BTN2A1 and BTN3A1 could promote granzyme B-mediated killing of $CD19^+$ lymphoma cells when co-cultured with $V\gamma9V\delta2^+$ T cells (31). Also, CD200 expression in MCL indicated a better prognosis and was associated with CD23 expression, frequent immunoglobulin heavy chain variable region (IGHV) mutations, and the absence of SOX11 expression (32,33). The majority of MCL patients had no or low expression of PD-1 and PD-L1 (14), while co-culturing of primary MCL cells with T-cells could induce PD-L1 surface expression (34). The generation of Tregs, which is a key role in the pathogenesis of follicular lymphoma, was associated with inducible costimulator (ICOS)/ ICOS Ligand (ICOSL) engagement (35). *IL2RB*, which is regarded as a hub gene, might be related to the pathogenesis and prognosis of MCL, as determined by the top-weighted network analysis performed in the GSE93291 dataset (6). *TNFRSF9* and its ligand *TNFSF9* were applied to trigger innate immune activation, involving therapies such as chimeric antigen receptor (CAR) T-cells and bispecific T-cell engagers in MCL and other B-cell lymphomas (36). Therefore, further investigations are needed to examine how the immune checkpoint molecules contribute to the pathogenesis of MCL and evaluate the value of these molecules.

A series of prognostic genes in MCL have been identified (5-7). However, the clinical application of these potential biomarkers as new targets in MCL treatment requires further exploration. In this study, we selected six DEGs (*LGALS2*, *LAMP3*, *ICOS*, *FCAMR*, *IGFBP4*, and *C1QA*) in two MCL clusters, which are associated with OS, to establish an efficient prognostic risk score model. Poor OS was related to increased *IGFBP4* and *C1QA* expression, while the worse prognosis was more likely to occur with low *LGALS2*, *LAMP3*, *ICOS*, and *FCAMR* expression. Also, patients with higher prognostic model risk scores had a markedly poor prognosis. The six prognostic genes directly and indirectly participated in the immune response in numerous tumors, for instance, *LGALS2* in triple-negative breast cancer (37), *LAMP3*+ dendritic cells in nasopharyngeal carcinomas (38), *ICOS* in the generation of Tregs in follicular lymphoma (35), *FCAMR* in lung squamous cell carcinoma (39), *IGFBP4* in ewing's sarcoma (40), *C1QA* in skin cutaneous melanoma (41). A previous study has suggested that *IGFBP4* is associated with poor outcomes in glioblastoma (42). Interestingly, in diffuse large B cell lymphoma (DLBCL) patients, the *C1qA*[276] polymorphism of the A/A allele is an independent favorable prognostic factor for rituximab plus cyclophosphamide, doxorubicin, vincristine, and prednisone (R-CHOP) as first-line therapy (43), while the expression level of *LGALS2* was not associated with OS but was lower in tumors than in normal samples (44). *LAMP3* is over-expressed in various tumors and is correlated with the poor or good prognosis of different patients (45). The different prognostic effects of these genes might relate to the different types of tumors, although their exact roles and mechanisms in MCL should be further explored.

We also performed Pearson's correlation analysis to assess the relative immune cells and immune checkpoint molecules of the above six prognostic genes. Most types of immune cells were positively correlated with the genes, including activated $CD8^+$ T cells, effector memory $CD8^+$ T cells, natural killer T cells, etc. Meanwhile, effector memory $CD4^+$ T cells and γδT cells exhibited a negative correlation with *IGFBP4*, and immature B cells were negatively correlated with *C1QA*. It is known that γδT cells can produce abundant cytokines and exert a therapeutic response against infection, autoimmunity, and cancer (46). The modulation of immune cells correlated with the six prognostic genes might explain the regulatory mechanisms in the TME of MCL to some extent. As for the immune checkpoint molecules, *ICOS*, *CD200*, *TNFRSF9*, *IL2RB*, *CD274*, and *BTN3A1* displayed significantly positive correlations with the whole six prognostic genes. Taken together, these findings suggested that the accommodation of immune checkpoint molecules might participate in the pathogenesis of MCL.

Conclusions

In conclusion, we screened four immune-related hub genes

(*CD247*, *CD3E*, *CD4*, and *GATA3*) in MCL, which were mainly enriched in the T-cell receptor signaling pathway and exhibited lower expression in tumors compared with normal samples. Subsequently, we recognized two MCL molecular clusters based on the hub genes. Patients in cluster 2 had a significantly worse OS compared with those in cluster 1; the hub genes were down-regulated, a variety of activated immune effector cells declined, and the majority of immune checkpoint molecules decreased. Moreover, we established an efficient prognostic risk score model using six prognostic genes (*LGALS2*, *LAMP3*, *ICOS*, *FCAMR*, *IGFBP4*, and *C1QA*) that were differentially expressed between the two MCL clusters. Patients with higher prognostic model risk scores had a significantly poorer prognosis. Although several biomarkers for the prognosis of MCL patients have been reported, few researches focused on the immune-related prognostic genes and the prognostic model developed by the DEGs of immune-related molecular clusters of MCL. This study suggested that these immune-related hub genes, the modulated immune cells, and the immune checkpoint molecules might be involved in oncogenesis and could be prognostic biomarkers in MCL. These immune-related biomarkers (four immune-related hub genes, six prognostic genes, and the relative molecules) will enrich the prognostic scoring system of MCL and provide preliminary basis for the clinical application of immunotherapy, including the immune checkpoint blockade therapies.

Further research should be carried out to examine the regulatory mechanisms through which the immune-related hub genes contribute to tumorigenesis, verify the efficiency of the prognostic model in larger MCL cohorts, and explore potential therapeutic targets that enhance the effect of immunotherapy.

Acknowledgments

We are very grateful for the assistance from Professor Jian-Quan Chen in the Central Laboratory and Translational Medicine Research Center of the Affiliated Jiangning Hospital of Nanjing Medical University.

Funding: This study was supported by the Natural Science Foundation of Jiangsu Province for Youths (No. BK20180280); the Innovation and Entrepreneurship Foundation of Jiangsu Province for Doctor (No. JSSCBS20211612); the Science and Technology Development Foundation for Health of Nanjing (Nos. YKK21227 and YKK20200); the Youth Innovation Foundation of the Affiliated Jiangning Hospital of Nanjing Medical University (Nos. JNYYZXKY202021 and JNYYZXKY202121); the Scientific Research Foundation of the Affiliated Jiangning Hospital of Nanjing Medical University for PhD. (No. JNYYRC202101); and the Science and Technology Development for Social Undertakings Foundation of the Jiangning district in Nanjing (No. 2020SHSY0101).

Footnote

Reporting Checklist: The authors have completed the TRIPOD reporting checklist. Available at https://atm.amegroups.com/article/view/10.21037/atm-22-5815/rc

Conflicts of Interest: All authors have completed the ICMJE uniform disclosure form (available at https://atm.amegroups.com/article/view/10.21037/atm-22-5815/coif). The authors have no conflicts of interest to declare.

Ethical Statement: The authors are accountable for all aspects of the work in ensuring that questions related to the accuracy or integrity of any part of the work are appropriately investigated and resolved. The study was conducted in accordance with the Declaration of Helsinki (as revised in 2013).

References

1. Armitage JO, Longo DL. Mantle-Cell Lymphoma. N Engl J Med 2022;386:2495-506.
2. Herrmann A, Hoster E, Zwingers T, et al. Improvement of overall survival in advanced stage mantle cell lymphoma. J Clin Oncol 2009;27:511-8.
3. Eyre TA, Cheah CY, Wang ML. Therapeutic options for relapsed/refractory mantle cell lymphoma. Blood 2022;139:666-77.
4. Ladha A, Zhao J, Epner EM, et al. Mantle cell lymphoma and its management: where are we now? Exp Hematol

Oncol 2019;8:2.
5. Bomben R, Ferrero S, D'Agaro T, et al. A B-cell receptor-related gene signature predicts survival in mantle cell lymphoma: results from the Fondazione Italiana Linfomi MCL-0208 trial. Haematologica 2018;103:849-56.
6. Guo D, Wang H, Sun L, et al. Identification of key gene modules and hub genes of human mantle cell lymphoma by coexpression network analysis. PeerJ 2020;8:e8843.
7. Carreras J, Nakamura N, Hamoudi R. Artificial Intelligence Analysis of Gene Expression Predicted the Overall Survival of Mantle Cell Lymphoma and a Large Pan-Cancer Series. Healthcare (Basel) 2022;10:155.
8. Yi S, Yan Y, Jin M, et al. Genomic and transcriptomic profiling reveals distinct molecular subsets associated with outcomes in mantle cell lymphoma. J Clin Invest 2022;132:e153283.
9. Kraehenbuehl L, Weng CH, Eghbali S, et al. Enhancing immunotherapy in cancer by targeting emerging immunomodulatory pathways. Nat Rev Clin Oncol 2022;19:37-50.
10. Ansell SM, Lesokhin AM, Borrello I, et al. PD-1 blockade with nivolumab in relapsed or refractory Hodgkin's lymphoma. N Engl J Med 2015;372:311-9.
11. Li X, Cheng Y, Zhang M, et al. Activity of pembrolizumab in relapsed/refractory NK/T-cell lymphoma. J Hematol Oncol 2018;11:15.
12. Dufva O, Pölönen P, Brück O, et al. Immunogenomic Landscape of Hematological Malignancies. Cancer Cell 2020;38:380-399.e13.
13. Xu-Monette ZY, Zhou J, Young KH. PD-1 expression and clinical PD-1 blockade in B-cell lymphomas. Blood 2018;131:68-83.
14. Ameli F, Shajareh E, Mokhtari M, et al. Expression of PD1 and PDL1 as immune-checkpoint inhibitors in mantle cell lymphoma. BMC Cancer 2022;22:848.
15. Assis-Mendonça GR, Fattori A, Rocha RM, et al. Single nucleotide variants in immune-response genes and the tumor microenvironment composition predict progression of mantle cell lymphoma. BMC Cancer 2021;21:209.
16. Papin A, Tessoulin B, Bellanger C, et al. CSF1R and BTK inhibitions as novel strategies to disrupt the dialog between mantle cell lymphoma and macrophages. Leukemia 2019;33:2442-53.
17. Chen Z, Teo AE, McCarty N. ROS-Induced CXCR4 Signaling Regulates Mantle Cell Lymphoma (MCL) Cell Survival and Drug Resistance in the Bone Marrow Microenvironment via Autophagy. Clin Cancer Res 2016;22:187-99.
18. Lv H, Fei Y, Li W, et al. A novel clinical immune-related prognostic model predicts the overall survival of mantle cell lymphoma. Hematol Oncol 2022;40:343-55.
19. Gómez-Abad C, Pisonero H, Blanco-Aparicio C, et al. PIM2 inhibition as a rational therapeutic approach in B-cell lymphoma. Blood 2011;118:5517-27.
20. Espinet B, Ferrer A, Bellosillo B, et al. Distinction between asymptomatic monoclonal B-cell lymphocytosis with cyclin D1 overexpression and mantle cell lymphoma: from molecular profiling to flow cytometry. Clin Cancer Res 2014;20:1007-19.
21. Scott DW, Abrisqueta P, Wright GW, et al. New Molecular Assay for the Proliferation Signature in Mantle Cell Lymphoma Applicable to Formalin-Fixed Paraffin-Embedded Biopsies. J Clin Oncol 2017;35:1668-77.
22. Yan W, Li SX, Wei M, et al. Identification of MMP9 as a novel key gene in mantle cell lymphoma based on bioinformatic analysis and design of cyclic peptides as MMP9 inhibitors based on molecular docking. Oncol Rep 2018;40:2515-24.
23. Dexiu C, Xianying L, Yingchun H, et al. Advances in CD247. Scand J Immunol 2022;96:e13170.
24. Wu W, Zhou Q, Masubuchi T, et al. Multiple Signaling Roles of CD3epsilon and Its Application in CAR-T Cell Therapy. Cell 2020;182:855-71.
25. Lisco A, Ye P, Wong CS, et al. Lost in Translation: Lack of CD4 Expression due to a Novel Genetic Defect. J Infect Dis 2021;223:645-54.
26. de Pádua Covas Lage LA, Brito CV, Levy D, et al. Diagnostic and prognostic implications of tumor expression of the GATA-3 gene in nodal peripheral T-cell lymphoma (nPTCL): Retrospective data from a Latin American cohort. Leuk Res 2022;114:106794.
27. Tosolini M, Algans C, Pont F, et al. Large-scale microarray profiling reveals four stages of immune escape in non-Hodgkin lymphomas. Oncoimmunology 2016;5:e1188246.
28. Zhang S, Jiang VC, Han G, et al. Longitudinal single-cell profiling reveals molecular heterogeneity and tumor-immune evolution in refractory mantle cell lymphoma. Nat Commun 2021;12:2877.
29. Zhang XY, Xu J, Zhu HY, et al. Negative prognostic impact of low absolute CD4(+) T cell counts in peripheral blood in mantle cell lymphoma. Cancer Sci 2016;107:1471-6.
30. Rodrigues JM, Nikkarinen A, Hollander P, et al. Infiltration of CD163-, PD-L1- and FoxP3-positive cells adversely affects outcome in patients with mantle cell lymphoma independent of established risk factors. Br J

Haematol 2021;193:520-31.
31. Lai AY, Patel A, Brewer F, et al. Cutting Edge: Bispecific γδ T Cell Engager Containing Heterodimeric BTN2A1 and BTN3A1 Promotes Targeted Activation of Vγ9Vδ2+ T Cells in the Presence of Costimulation by CD28 or NKG2D. J Immunol 2022;209:1475-80.
32. Hu Z, Sun Y, Schlette EJ, et al. CD200 expression in mantle cell lymphoma identifies a unique subgroup of patients with frequent IGHV mutations, absence of SOX11 expression, and an indolent clinical course. Mod Pathol 2018;31:327-36.
33. Saksena A, Yin CC, Xu J, et al. CD23 expression in mantle cell lymphoma is associated with CD200 expression, leukemic non-nodal form, and a better prognosis. Hum Pathol 2019;89:71-80.
34. Harrington BK, Wheeler E, Hornbuckle K, et al. Modulation of immune checkpoint molecule expression in mantle cell lymphoma. Leuk Lymphoma 2019;60:2498-507.
35. Le KS, Thibult ML, Just-Landi S, et al. Follicular B Lymphomas Generate Regulatory T Cells via the ICOS/ICOSL Pathway and Are Susceptible to Treatment by Anti-ICOS/ICOSL Therapy. Cancer Res 2016;76:4648-60.
36. Watanabe T. Approaches of the Innate Immune System to Ameliorate Adaptive Immunotherapy for B-Cell Non-Hodgkin Lymphoma in Their Microenvironment. Cancers (Basel) 2021;14:141.
37. Ji P, Gong Y, Jin ML, et al. In vivo multidimensional CRISPR screens identify Lgals2 as an immunotherapy target in triple-negative breast cancer. Sci Adv 2022;8:eabl8247.
38. Peng WS, Zhou X, Yan WB, et al. Dissecting the heterogeneity of the microenvironment in primary and recurrent nasopharyngeal carcinomas using single-cell RNA sequencing. Oncoimmunology 2022;11:2026583.
39. Li N, Wang J, Zhan X. Identification of Immune-Related Gene Signatures in Lung Adenocarcinoma and Lung Squamous Cell Carcinoma. Front Immunol 2021;12:752643.
40. Zhou Y, Xu B, Wu S, et al. Prognostic Immune-Related Genes of Patients With Ewing's Sarcoma. Front Genet 2021;12:669549.
41. Yang H, Che D, Gu Y, et al. Prognostic and immune-related value of complement C1Q (C1QA, C1QB, and C1QC) in skin cutaneous melanoma. Front Genet 2022;13:940306.
42. Zhong Z, Xu X, Han S, et al. Comprehensive Analysis of Prognostic Value and Immune Infiltration of IGFBP Family Members in Glioblastoma. J Healthc Eng 2022;2022:2929695.
43. Jin X, Ding H, Ding N, et al. Homozygous A polymorphism of the complement C1qA276 correlates with prolonged overall survival in patients with diffuse large B cell lymphoma treated with R-CHOP. J Hematol Oncol 2012;5:51.
44. Ma C, Li H. Hub Gene and Its Key Effects on Diffuse Large B-Cell Lymphoma by Weighted Gene Coexpression Network Analysis. Biomed Res Int 2021;2021:8127145.
45. Alessandrini F, Pezzè L, Ciribilli Y. LAMPs: Shedding light on cancer biology. Semin Oncol 2017;44:239-53.
46. Muro R, Takayanagi H, Nitta T. T cell receptor signaling for γδT cell development. Inflamm Regen 2019;39:6.

(English Language Editor: A. Kassem)

Cite this article as: Zhang W, Shi JN, Wang HN, Zhang T, Zhou X, Zhang HM, Zhu F. Identification of immune-related genes and development of a prognostic model in mantle cell lymphoma. Ann Transl Med 2022;10(24):1323. doi: 10.21037/atm-22-5815

